X-ray diffraction measurement of the linear thermal expansion coefficients of WCoB in the range 300 to 973 K

Orthorombic WCoB (ordered $PbCl_2$ structure, Type E-TiNiSi) has been found in the ternary system tungsten–cobalt–boron [1, 2]. Its crystal structure is described by the space group Pnma, the lattice constants being $a = 0.5724$ nm, $b = 0.3240$ nm and $c = 0.6632$ nm [3]. In some earlier papers [4, 5] it was shown that high-temperature treatment of tungsten carbide–cobalt hard alloys in TiB_2 media leads to the formation of a surface diffusion coating which contains WCoB. Hard alloy carbide cutting tools coated in this way have better performance due to enhancement of the wear resistance and their resistance to high-temperature oxidation [5, 8].

The diffusion coating of this type is heterogeneous. It consists of a number of crystallites of different phases. More detailed studies of the correlation between their physical properties could be of special importance with a view to enhancing the wear resistance of cutting tools. In this connection, the thermal expansion of WCoB was of primary interest, since the wear resistance of the coating obviously reflects the degree of matching of the thermal expansion coefficients of the different phases.

Polycrystalline WCoB samples were prepared by crystallization from cobalt-rich melts of the corresponding powdery components. Compacted pellets of mixed tungsten, cobalt and boron powders were melted in an induction furnace under argon atmosphere. The temperature of the melt was slowly reduced from 1880 K to room temperature for 24 h. Under these conditions primary crystallization of WCoB was observed [3]. Selective dissolving in boiling HCl was used to isolate the polycrystalline powder of WCoB from the co-products. The X-ray powder diffraction analyses of the end product showed the presence of single-phase WCoB.

Attempts were also made to prepare larger single crystals. Pressed pellets of the cobalt-rich powder mixture of the components were out-gased (at 10^{-4} torr) in the induction furnace vacuum chamber. The system was then filled with argon and the pellets were melted by increasing the temperature at a rate of $50\,K\,h^{-1}$. After a homogenization period lasting several hours the temperature of the melt was slowly decreased at a rate of 1 to $2\,K\,h^{-1}$. Before the start of crystallization, a tungsten wire attached to the water-cooled pulling shaft was dipped into the melt and pulled out at a linear speed of $0.3\,mm\,h^{-1}$. The drop-like matrix pulled in this way contained a considerable number of large WCoB single crystals, some of them having dimensions of 1 × 1.5 × 3 mm. The single crystals were isolated from the matrix by selective dissolution of the co-products, as in the previous case. X-ray Weissenberg diffraction patterns and oscillation diffraction patterns showed the preferred direction of crystal growth to be (0 1 0). For high-temperature powder diffraction measurements, several large single crystals were ground in an agate mortar, the powder was then pressed into pellets (1 mm thickness, 10 mm diameter) and annealed at 1170 K for 24 h in an argon atmosphere. No change in the phase composition was observed after the thermal treatment.

X-ray diffraction patterns were observed using a Seimens diffractometer using CuKα monochromatic radiation and a scintillation counter. The diffraction spectra were recorded at a constant speed using a chart recorder. The samples were mounted in a continuous helium-flow high-temperature attachment. The heating element was a tantalum resistive band, with a profile designed in such a way as to maintain a constant geometry of the experiment. The heater also played the role of a sample holder. The temperature was controlled by means of a Pt–PtRh thermocouple and kept constant to within an accuracy of ± 2 K. The powder diffraction pattern lines seen at room temperature were indexed according to published [3] values of the cell parameters. Accurate values were calculated by minimizing the difference between the observed and calculated $\sin^2\theta$ values, where θ is the Bragg angle, for all lines having Bragg angles up to $\theta = 60^\circ$. The cell parameters at 12 different temperatures in the range 300 to 973 K were calculated from the diffraction lines with Bragg angles $30^\circ \leqslant \theta \leqslant 55^\circ$. A routine least-squares fit computer program, written in the Institute of Mineralogy, University of Bonn, was used for the calculations. The accuracy of the cell dimensions was within the limits of ± 0.0002 nm for a and c and ± 0.0001 nm for b. The high-temperature measurements carried out several times at increasing and decreasing temperatures showed a good repro-

0022–2461/81/113218–3$02.30/0

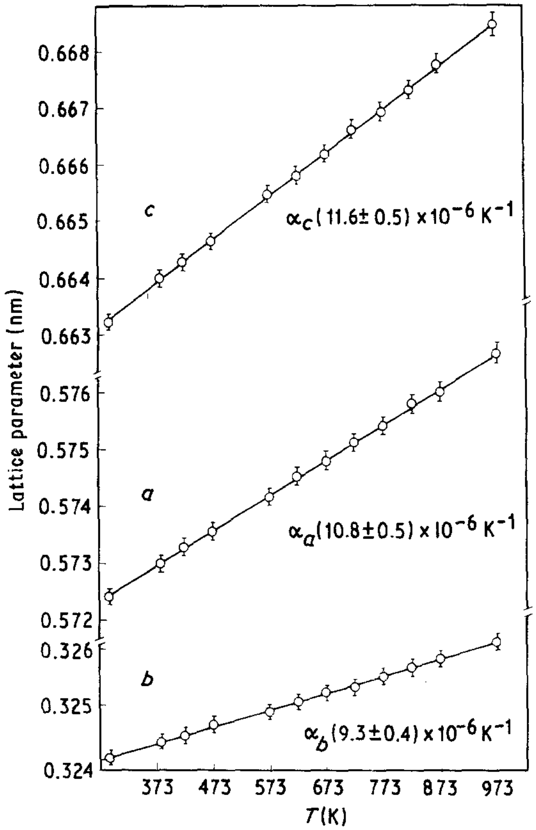

Figure 1 Temperature dependence of the lattice parameters of E–WCoB.

TABLE I Data of inter-atomic distances

Interatomic distances in WCoB, from [3]			Interatomic Me–Me, Me_1–Me_2 distances from [9] (nm)	Me–B distances in W_2B, [10, 11] (nm)
Atom	Neighbours	Distance (nm)		
W	2W	0.2829		
	2W	0.3035	0.2816	
	2W	0.3240		
	2Co	0.2588	0.2660	
	2Co	0.2619		
	1Co	0.2628		
	1Co	0.2649		
	2B	0.2350		0.2380
	2B	0.2362		
	1B	0.2494		
Co	2W	0.2588	0.2660	
	2W	0.2619		
	1W	0.2628		
	1W	0.2649		
	2Co	0.2456	0.2504	
	2Co	0.3240		
	2B	0.2122		0.2150
	1B	0.2146		
	1B	0.2230		
B	2W	0.2350		0.2380
	2W	0.2362		
	1W	0.2494		
	2Co	0.2122		0.215
	1Co	0.2146		
	1Co	0.2230		

ducibility. The temperature dependences of the cell parameters and the corresponding values of the thermal expansion coefficients are given in Fig. 1.

As is seen in Fig. 1, the linear thermal expansion coefficients along the three principal crystallographic directions have different values. The explanation of this fact can be given in terms of the bonding features in the solid.

In the crystal lattice of the E-phase all the atoms are situated in the mirror planes perpendicular to the *b*-axis at $y = 1/4$ and $y = 3/4$, forming two-dimensional nets of pentagons, centred in the *b* projection by the W atoms. Boron atoms have 9 nearest neighbours: 4W and 2Co form a distorted trigonal prism with a boron atom in the centre; 2Co and 1W are outside the rectangular prismatic faces in the same plane as the central atom. The inter-atomic distances list (Table I) supports the assumption that the interactions Co–Co and W–W are weaker than those in the corresponding metal lattices [3]. On the other hand, the interaction of the boron atom with metal atoms of the under- and overlying nets is stronger than the interaction with the nearest metal atoms from the same net. The last two details could explain the observed anisotropy of the thermal expansion coefficient. A similar temperature behaviour was observed for the iron boride Fe_2B [6].

The absolute values of the thermal expansion coefficients, α, are also of special importance. WCoB shows a considerably stronger expansion with temperature than does tungsten carbide ($\alpha_{WC} = 3.8\text{–}3.9 \times 10^{-6}\,K^{-1}$ [7]). Thus, in a composite material, which can be regarded as consisting of support and coating, the thermal deformation will give rise to strains. The magnitude of these strains, generally, is proportional to the difference in the thermal expansion coefficients of the support and the coating. In particular, the strains in the coating may be dependent on its morphology, i.e. on whether it is an "island" formation or a continuous film. In the first case practically strain-free support and coating could be expected; in the second case the coating and the support will also be strain-affected.

Acknowledgements

Experiments were carried out in the Institute of Mineralogy, University of Bonn, as part of a joint research project with the Bulgarian Academy of Sciences. The financial support of the Deutsche Forschungsgemeinschaft is gratefully acknowledged. Thanks are also due to the members of the Institute of Mineralogy and especially to Dr Wallrafen.

References

1. H. HASCHKE, H. NOWOTNY and F. BENESOVSKY, *Mh. Chem.* 97 (1966) 1459.
2. YU. B. KUZ'MA, P. I. KRIPYAKEVICH and M. V. CHEPIGA, *Zh. Structur. Chem.* 9 (1968) 327.
3. W. JEITSCHKO, *Acta Cryst.* **B24** (1968) 930.
4. D. MERCURIO-LAVAUD, K. PETROV, P. PESHEV and Z. ZAKHARIEV, *J. Less-Common Met.* 67 (1979) 59.
5. P. PESHEV, Z. ZAKHARIEV and K. PETROV, *J. Less-Common Met.* 67 (1979) 351.
6. C. MAI, M. AYEL, G. MONNIER and R. RIVIERE, *C. R. Acad. Sci. Paris* 267D (1968) 987.
7. G. V. SAMSONOV and I. M. VINITSKII, "Tugoplavkie soedineniya" (Metalurgiya, Moskva, 1976) p. 212.
8. G. BLIZNAKOV, P. PESHEV and Z. ZAKHARIEV, *J. Less-Common Met.* 67 (1979) 511.
9. W. B. PEARSON, "The Crystal Chemistry of Metals and Alloys" (Wiley Interscience, New York, 1972) Chap. 4.
10. R. KIESSLING, *Acta Chem. Scand.* 1 (1947) 893.
11. T. BJURSTRÖM, *Ark. Kemi Min. Geol.* **11A(5)** (1933) 1.

Received 16 February
and accepted 26 March 1981

K. PETROV
Institute of General and Inorganic Chemistry,
Bulgarian Academy of Sciences,
1040 Sofia,
Bulgaria
G. WILL
Mineralogisches Institut der Universität Bonn,
Lehrstuhl für Mineralogie und Kristallographie,
D 5300 Bonn,
West Germany

Effect of voids on the electrical resistivity in lead zirconate–titanate ceramics

Lead zirconate–titanate (PZT) is an important ceramic material widely used for piezoelectric devices [1, 2]. Electrical conductivity which relates to the power loss of the devices is an important physical property. Previous investigators have only considered the resistivity problem from the standpoint of defect structure in PZT [3–5]. Because of differing fabrication techniques, complete densification is usually not achieved in ceramic materials. An understanding of the effects of voids or porosity on the electrical resistivity of PZT is necessary for a complete characterization of this property. Some work has been conducted to try to relate the ceramic microstructure of PZT to the other ferroelectric and piezoelectric properties [6–9].

The major problem encountered when studying the electrical properties of PZT is PbO loss during sintering. It has been reported that even a small amount of PbO loss from the system can cause appreciable differences in the electrical and physical properties [10]. Previous investigators attempted to control the grain size and porosity by varying the processing parameters, mainly the pressure, temperature, and time for hot-pressing and sintering. The PbO loss from the system is also affected by the process parameters. Therefore, the previous studies, while obtaining data on the effect of grain size and porosity, have not clearly demonstrated that the defect structure has remained constant. Holman and Fulrath [11] established the PbO activity for the $PbZrO_3$–$PbTiO_3$ system and determined the single-phase solid-solution width of the compounds in the system with temperature. Thus, a multi-phase packing powder technique was established that allowed reproducible processing of PZT compositions to a controlled and con-

0022–2461/81/113220–3$02.30/0